Metal oxide semiconductor nanomaterial for reductive debromination: Visible light degradation of polybrominated diphenyl ethers by Cu$_2$O@Pd nanostructures

Edward B. Miller[a], Elsayed M. Zahran[a,b], Marc R. Knecht[a], Leonidas G. Bachas[a,*]

[a] Department of Chemistry, University of Miami, Coral Gables, Florida 33146, United States
[b] Applied Organic Chemistry Department, National Research Centre, Egypt

ABSTRACT

Polybrominated diphenyl ethers (PBDEs), which have found extensive use as flame-retarding additives to many polymer materials, are now environmentally ubiquitous and persistent pollutants that present potential health risks to humans and wildlife. Herein, we report for the first time the use of metal oxide semiconductor nanostructures for photocatalytic reductive debromination of PBDEs using visible light. Well-defined cubic Cu$_2$O crystals, surface-decorated with Pd nanoparticles, were prepared via a hydrothermal approach. The Cu$_2$O@Pd demonstrated light-activated tandem photocatalysis, in which Cu$_2$O produces H$_2$ from H$_2$O under visible light irradiation; the evolved H$_2$ is subsequently activated by Pd to achieve the reductive hydrodehalogenation of the PBDE. Cu$_2$O@Pd demonstrated effective debromination of 2,2′,4,4′-tetrabromodiphenyl ether (BDE-47), one of the PBDEs of greatest environmental concern, with initial pseudo-first-order rate constant of 0.21 h^{-1}. It is shown that the reaction proceeds via a reductive mechanism with preferential debromination at the *para* positions. Reaction rates for various monobromo- and dibromo-congeners were evaluated, confirming that the debromination order of preference is *para > meta >> ortho*, which is opposite to the order reported for direct photolysis. We conclude that Cu$_2$O@Pd is a promising photocatalyst for reductive dehalogenation of halogenated organic compounds.

© 2017 Elsevier B.V. All rights reserved.

1. Introduction

Polybrominated diphenyl ethers (PBDEs) are a group of highly stable compounds comprised of 209 congeners, several of which had been employed extensively as chemical flame-retarding agents added to flammable materials such as plastics and textiles used in a wide range of products [1–3]. As additive flame-retardants, PBDEs were mixed with, but not chemically bound to, polymers of a product; the latter is the case with reactive flame-retardants. As such, PBDEs can be readily released into the environment from discarded products and have become a ubiquitous environmental pollutant [4–10]. Widespread distribution of these compounds in the environment is of particular concern, because they are known to act as endocrine disruptors [11–13], impair neurobehavioral development [14], and could cause DNA damage [15]. Because of the potential hazards associated with PBDE exposure, many of these compounds have recently been banned, whereas the remaining ones have been voluntarily phased-out in the United States [16,17]. Nevertheless, the extensive use of these compounds in the past translates into a large reservoir in the environment [18,19]. On account of their widespread contamination, environmental persistence, and health hazard, it is important to develop new and effective approaches for PBDE mitigation.

A number of natural environmental processes are known to degrade PBDEs. Several bacterial [20–24] and fungal [25] species have been identified that are capable of feeding upon and breaking down PBDEs. While biodegradation occurs naturally, it proceeds very slowly [24]. It should be noted that in the case of oxidative biodegradation processes, many of the products formed, including polybrominated dibenzofurans (PBDFs) and hydroxylated polybrominated diphenyl ethers (HO-PBDEs), could be more hazardous than the parent compounds [26].

Several non-biological degradation methods, principally photolysis [27], dehalogenation by zero-valent iron [28], and photocatalytic degradation by TiO$_2$ [29], have been proposed for the remediation of PBDEs [30,31]. Photolysis can occur under UV irra-

diation, which leads to either homolytic or heterolytic cleavage of a C—Br bond or a C—O bond, or in a ring-closure with the elimination of HBr to produce PBDFs. For instance, the prevailing mechanism in the presence of a strongly-nucleophilic solvent such as water, is heterolytic C—Br cleavage [30]. This eventually results in formation of the more hazardous HO-PBDEs through nucleophilic substitution under aqueous conditions. PBDEs also absorb in the UV-A region of the spectrum [27] and, except under special conditions, visible light is insufficient for their photolysis. The exception recently reported by Sun and co-workers utilizes carboxylate anions, which form a visible-light-absorbing halogen bond complex with the PBDE, facilitating its photolysis at a longer wavelength [32]. In this case, however, the photolysis of decabromodiphenyl ether (BDE-209) did not result in the degradation of the material beyond the tetra-bromodiphenyl ether congeners.

The photolytic degradation of PBDEs generally takes place in a stepwise fashion, with the loss of one bromine atom at a time. As such reactions proceed, however, the removal of each successive bromine atom becomes more difficult, where the fewer bromine substituents there are on the molecule, the stronger the C-Br bonds become, as evidenced by the shift in absorbance λ_{max} to shorter wavelengths. Density Functional Theory (DFT) calculations indicate that removal of each successive bromine atom increases the stability of the molecule by about 22 kJ/mol after correction for differences in bromination patterns [33]. This results in a preponderance of congeners with an intermediate number of bromines that are resistant to further debromination, most notably the pentabromo- and tetrabromo- congeners, BDE-99 and BDE-47, respectively [34–36]. Although TiO$_2$-based materials have demonstrated effective oxidative photocatalytic degradation of PBDEs in organic solvents [30], this reaction still suffers from two major drawbacks: oxidation can produce highly toxic by-products, and UV irradiation is required as TiO$_2$ is a wide band gap semiconductor. Reductive debromination using TiO$_2$@Pd [37] or CuO/TiO$_2$ [38,39] nanocomposite photocatalysts was recently reported. Although these materials resulted in rapid reductive debromination, they still suffer from two major drawbacks: they need UV irradiation and, moreover, the solvent systems consisted of 70–100% methanol, an environmentally unfriendly requirement. An ideal photocatalyst would make use of the abundant visible solar output to drive a non-oxidative degradation mechanism using only environmentally benign solvents.

Reductive debromination by H$_2$ generated through reaction of nanoscale zero-valent iron (nZVI) or by palladium/iron bimetallic nanomaterials (nZVI@Pd) with water has been investigated as an alternative approach that avoids the formation of toxic oxidative products [30]. Zhuang et al. showed that adding Pd to the surface of nZVI both increases the reaction rate and alters the mechanism to produce different products; the nZVI@Pd particles favor removal of *para* bromines, while pristine nZVI favors *meta*- and *ortho*-debromination [40]. A key drawback to this method, however, is that the production of H$_2$ from water is a stoichiometric reaction in which the nZVI is oxidized. This results in the formation of iron oxides/hydroxides on the surface of the nZVI, thus adversely impacting the rate of debromination due to the lack of H$_2$ production from the oxidized surface [41]. As such, a catalytic reaction based upon sustainable materials, consistent with the principles of Green Chemistry [42], has been much sought.

We recently introduced a novel composite material consisting of Cu$_2$O cubes, surface-decorated with Pd nanoparticles, that has been shown to perform as a tandem photocatalyst in the reductive dechlorination of polychlorinated biphenyls (PCBs) [43]. In this material architecture, Cu$_2$O nanomaterials are well established p-type semiconductors which are able to generate H$_2$ via the photocatalytic water splitting reaction [44], while the Pd particles on the Cu$_2$O cubes provide localized catalytic sites for the hydrode-

halogenation reaction in the vicinity of the photogenerated H$_2$ [43]. In this approach, the production of H$_2$ via photocatalytic proton reduction on the surface of Cu$_2$O crystals is achieved by light activation. Subsequently, this H$_2$ is activated on the surface of Pd nanoparticles to drive the reductive dehalogenation reaction. Furthermore, the direct band gap of Cu$_2$O is such that visible light irradiation could be used for exciton generation [44]. Use of this material provides significant advantages over other methods in that it could drive the dehalogenation reaction sustainably using renewable resources, namely sunlight and water.

Herein, we report the visible-light driven reductive debromination of PBDEs using a non-titania-based narrow band gap metal oxide semiconductor nanocomposite photocatalyst. Cubic Cu$_2$O particles were prepared by a simple hydrothermal process and subsequently surface-decorated with Pd nanoparticles via galvanic replacement. The resulting Cu$_2$O@Pd multicomponent material was then used as photocatalyst for the reductive debromination of various congeners of PBDEs under visible light. The results show that rapid degradation of BDE-47 is achieved, and the sequence of debromination products is consistent with the reductive mechanism. It was found that the catalyst is most effective in debrominating PBDEs at the *para* positions, whereas direct photolysis is known to debrominate most readily at *ortho* and *meta* positions [31]. Insight into the mechanism of this reaction and a comparison to the direct photolysis of PBDEs were investigated.

2. Experimental details

2.1. Materials and equipment

All reagents were used as received without further purification. BDE-47 (99.5%) was purchased from Chem Service (West Chester, PA). BDE-3 (99%), BDE-15 (99%), glucose (anhyd., 99%), and ethyl acetate (99%) were obtained from Alfa Aesar (Ward Hill, MA). BDE-1, BDE-4, and BDE-8 were purchased from AccuStandard (New Haven, CT), as were reference standard solutions (each 50 µg/mL in isooctane) of BDE-17 and BDE-28. Dibenzofuran (100 µg/mL in methanol) was supplied by Ultra Scientific (Kingstown, RI). Diphenyl ether (>99%) was obtained from TCI (Portland, OR). BDE-2, polyvinylpyrrolidone (avg. MW = 29 kDa), and sodium citrate (ACS) were from Sigma-Aldrich (St. Louis, MO). Sodium carbonate (anhyd., ACS) and hexanes (HR-GC grade) were supplied by EMD (Gibbstown, NJ). Palladium acetate (47.5% Pd) was purchased from Acros Organics (Morris Plains, NJ), copper sulfate pentahydrate (ACS) from BDH (Radnor, PA), and 1,2-dibromobenzene from Oakwood Chemical (West Columbia, SC). Absolute ethanol was obtained from Pharmco Aaper (Shelbyville, KY) and ethanol (95%) from Decon Labs (King of Prussia, PA). Ultra-high-purity N$_2$ was purchased from Airgas (Miami, FL). Ultra-pure water (18 MΩ) was produced by a Barnstead E-Pure system (Thermo Fisher Scientific, Waltham, MA).

Scanning electron microscopy (SEM) and transmission electron microscopy (TEM) were employed in the characterization of the Cu$_2$O and Cu$_2$O@Pd materials using a Philips XL30 field-emission environmental SEM equipped with an Oxford energy-dispersive X-ray detector and a JEOL JEM-1400 TEM, respectively. SEM experiments were performed at 20 kV, while TEM experiments were conducted at 80 kV. Debromination reactions were done in a photochemical safety cabinet (Ace Glass, Vineland, NJ, model #7836-20) under irradiation by a 450 W medium-pressure mercury-vapor lamp (Ace Glass #7825-34, light intensity = 60 mW/cm^2). Reaction progress was monitored by GC/MS (Agilent 5975C GC/MS with HP-5MS column: 30 m length, 0.250 mm ID, 0.25 µm film thickness, Santa Clara, CA) using 1,2-dibromobenzene as an internal standard [41,43].
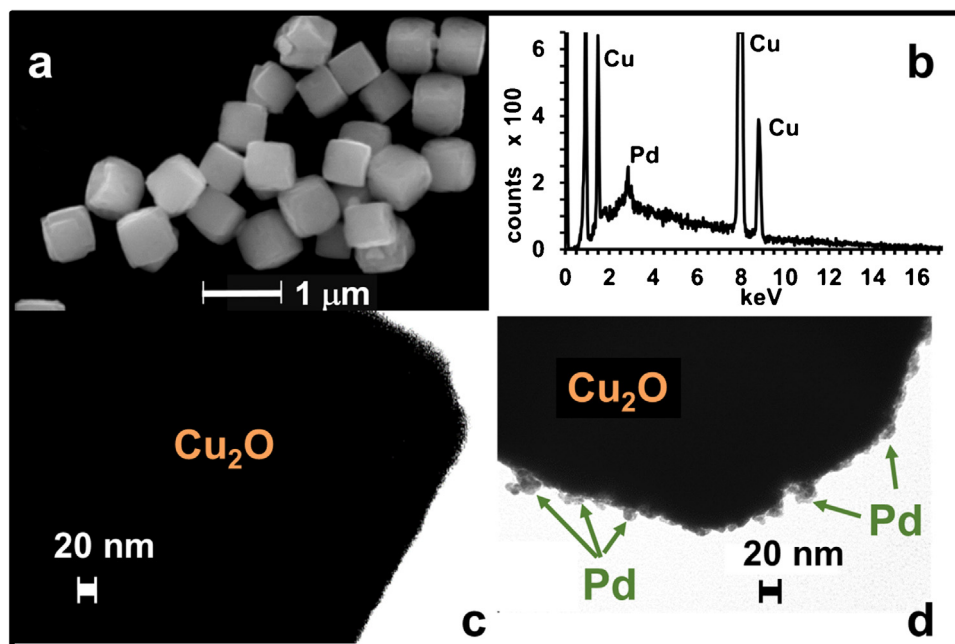
Fig. 1. (a) SEM image of Cu_2O cubes; (b) EDS analysis of $Cu_2O@Pd$; (c) TEM image of Cu_2O; (d) TEM image of $Cu_2O@Pd$ showing Pd surface decoration.

2.2. Synthesis of $Cu_2O@Pd$

Cu_2O was prepared according to the method described by Zahran et al. [43]. Briefly, 3.0 g polyvinylpyrrolidone (PVP) was dissolved in 210 mL of a 0.032 M aqueous $CuSO_4$ solution. The mixture was stirred for 15 min, after which 40 mL of 0.37 M aqueous sodium citrate and 0.61 M sodium carbonate were added dropwise while stirring continued. During this addition, the color of the solution changed from light transparent aqua to opaque light turquoise, and finally to a transparent deep blue. The mixture was stirred for another 15 min, whereupon 50 mL of 1.4 M glucose solution was slowly added. At this point, the stir bar was removed, and the flask was closed with a ground glass stopper and covered with aluminum foil to exclude light. The flask was then submerged in a water bath at 80 °C for 2 h. The resulting dark orange-red product was collected by filtering the mixture through a 200-nm track-etched polycarbonate membrane, washed with water followed by ethanol, and dried overnight *in vacuo* at 60 °C. The dried Cu_2O (1.2 g, from 3 batches combined) was suspended in 800 mL absolute ethanol, to which 140 mg of palladium(II) acetate in 8 mL ethyl acetate was added. The mixture was stirred overnight in the dark. The resulting $Cu_2O@Pd$ was collected by filtration, washed, and dried as above.

2.3. Photocatalytic debromination of brominated diphenyl ethers

BDE-47 (50 mL, 15.0 μM) in a 50:50 (v/v) ethanol/water solution was added to 50 mg of $Cu_2O@Pd$ in a 60 mL borosilicate glass vial with a silicone septum cap and magnetic stir bar. The vial was sealed, flushed with dry ultra-high purity N_2 and sonicated for 5 min. It was then placed on a stir plate in a light cabinet at a distance of 11 cm from a water-cooled 450 W medium-pressure mercury-vapor lamp. At selected time points, 500 μL aliquots were taken and combined with equal volumes of high-resolution-GC-grade hexanes in 2 mL vials. The vials were agitated for 1 h on a vortexer to extract the organic products into the hexane layer. One-hundred-microliter samples of the hexane extracts were spiked with 15 μL of 18.3 μM 1,2-dibromobenzene in hexanes as an internal standard and analyzed using GC/MS. The extraction recovery was assessed by adding biphenyl as a surrogate standard (10 μM final concen-

tration) to the reaction solution prior to irradiation and was found thereafter to be $96.7 \pm 4.4\%$ (n = 3).

The same procedure was followed for each of the other PBDEs (BDE-1, 2, 3, 4, 8, and 15). To explore the effect of UV *vs.* visible irradiation on the debromination of BDE-47, the vials were wrapped with a flexible polyester UV filter film (400 nm long-pass filter, Edmund Optics #39-426). All reactions were performed at least three times each, unless mentioned otherwise.
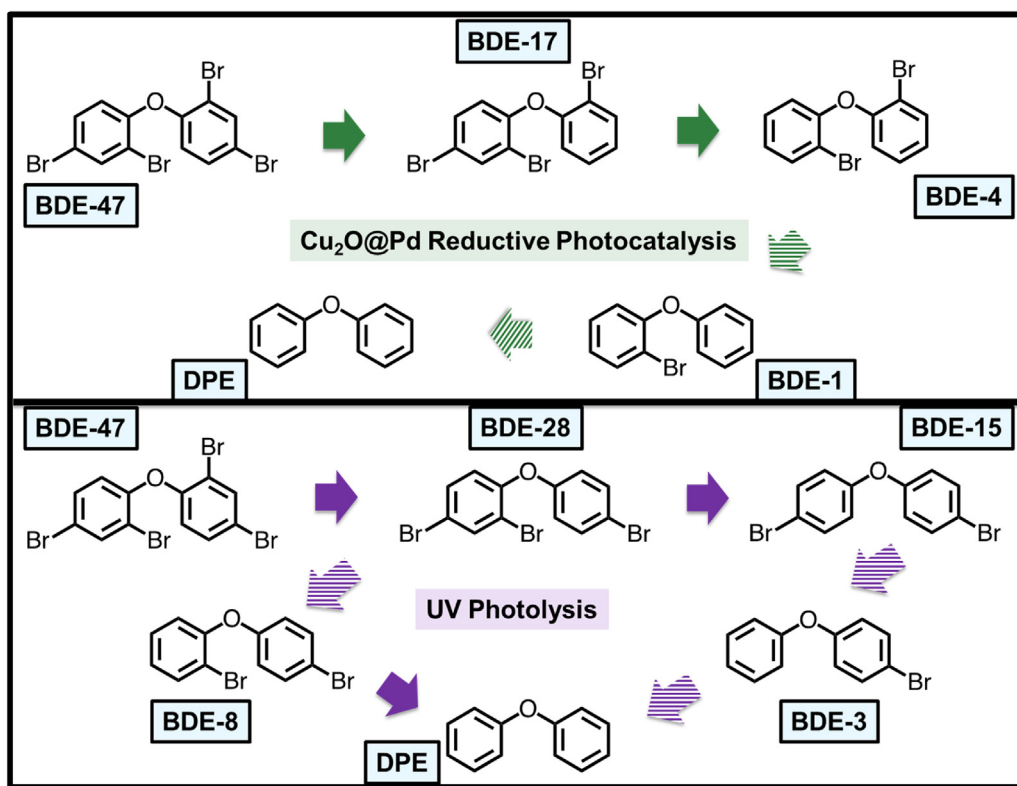
3. Results and discussion

3.1. Characterization of $Cu_2O@Pd$

Multicomponent materials based on copper(I) oxide cubes decorated with palladium nanoparticles were prepared following the procedure outlined by Zahran *et al.*[43]. As shown by the scanning electron microscopy (SEM) image in Fig. 1a, well-defined Cu_2O cubes were prepared with average size of 560 ± 110 nm (n = 100). Pd nanoparticles were subsequently deposited on the surface of Cu_2O cubes by galvanic replacement. The energy-dispersive X-ray spectroscopy (EDS) spectrum in Fig. 1b shows a peak at 2.8 keV for the Pd Lα X-ray line with the palladium content in the multicomponent material being 3.6 ± 0.4 wt%. TEM images of Cu_2O before and after palladization (Fig. 1c and d) show the Pd nanoparticles (∼7 nm) being uniformly distributed on the surface of Cu_2O. This material ensemble was found to be critical for the catalytic activity of Pd nanoparticle-decorated materials [41].

3.2. Reductive debromination of BDE-47

To demonstrate the reactivity of $Cu_2O@Pd$ in the photocatalytic debromination of polybrominated diphenyl ethers, 2,2′,4,4′-tetrabromodiphenyl ether (BDE-47) was selected (Scheme 1); BDE-47 is one of the congeners most commonly found in the environment and in human tissue samples, and is thus of great concern in terms of its potential hazards [1,45–47]. In addition, its symmetric structure with one *para-* and one *ortho-*bromine on each of the two benzene rings limits the number of potential debromination products and allows for insight into the debromination mechanism.

Scheme 1. Products of BDE-47 debromination. Upper pathway (green arrows) indicates product sequence in the presence of Cu$_2$O@Pd; lower pathway (purple arrows) corresponds to direct photolysis. Solid arrows show favored pathways. (For interpretation of the references to colour in this figure legend, the reader is referred to the web version of this article.)

As a further consideration, BDE-47 does not have adjacent bromine atoms on either ring, thus obviating alternative degradation pathways involving concerted elimination of adjacent bromines. Such mechanisms, shown by Zhuang *et al.* [40] to be benefitted by adjacent bromines, may partly contribute to some of the more rapid debromination reactions reported for BDE-209, the congener most studied in the literature [30]. However, since the predominant PBDEs in the environment do not have adjacent bromine atoms, we chose to use BDE-47 as the more realistic environmental model compound.

Accordingly, to explore the activity of the Cu$_2$O@Pd nanocrystals for photocatalytic debromination of PBDEs, 50 mg of the material was added to 50 mL of 15 μM (50%/50%) (EtOH/water) solution of BDE-47 under irradiation by a medium pressure mercury vapor lamp. Ethanol was added to enhance the solubility of BDE-47 in aqueous solution and to serve as a hole-scavenger in the photocatalytic water splitting reaction. Such conditions were shown previously to promote the reductive dechlorination of PCBs [43]. Batch reactions that were prepared in pure water or (50%/50%) (acetonitrile/water) solution demonstrated no activity after 20 h of light irradiation. Fig. 2 shows the photocatalytic debromination results of BDE-47 with Cu$_2$O@Pd nanostructured material. The first bromine was rapidly removed from one of the *para* positions, and within 5 h, there was a 50% reduction in the concentration of BDE-47 while generating a series of lesser-brominated products. The initial pseudo-first-order rate constant of this process is 0.21 h^{-1}, and the sequence of product formation (Scheme 1, upper pathway) is BDE-47 to BDE-17 (2,2′,4-tribromodiphenyl ether), followed by BDE-4 (2,2′-dibromodiphenyl ether). Generally, the reductive photodebromination of PBDEs proceeds via stepwise removal of one bromine substituent at a time, and is likely to take place through a homolytic pathway [30]. This is supported by the results shown in Fig. 2, where the tetrabromo-species disappeared first, fol-
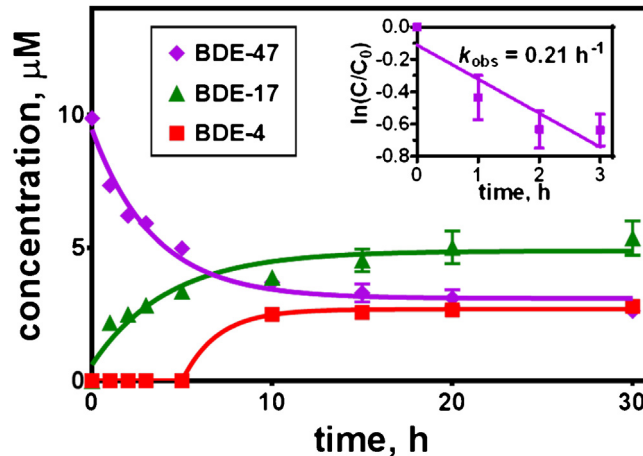

Fig. 2. Photodebromination reaction of BDE-47 under light irradiation with 1 mg/mL Cu$_2$O@Pd suspension. Inset shows ln(C/C$_0$) vs. time and indicates pseudo-first-order rate constant. Error bars represent standard error (n = 3).

lowed by the tribromo- and later the dibromo-congeners appearing in its place. Furthermore, no hydroxylated PBDE products were detected, indicating that a heterolytic process was unlikely. Non-catalytic photolysis is known to favor debromination at the *ortho* position [31], resulting in a product sequence formation pattern (Scheme 1, lower pathway) that includes BDE-28 (2,4,4′-tribromo-DPE) followed by BDE-15 (4,4′-dibromo-DPE). On the other hand, the Cu$_2$O@Pd catalyst drives debromination of BDE-47 preferentially at the *para* position, as evidenced by the observed product sequence formation. For comparison, Fig. S1 shows the result of direct photolysis of BDE-47 under the same light exposure conditions.

DFT calculations for the monobromodiphenyl ethers by Zeng et al. showed that the *para*-bromine of BDE-3 was 6 kJ/mol more stable than the *ortho*-bromine of BDE-1 [33]. Thus, in the direct photolysis of the C-Br bond, the result reported in the literature is as it would be expected: loss of bromine at the thermodynamically-favored *ortho* position [31]. The Cu$_2$O@Pd catalyzed reaction, however, depends on the interaction between the BDEs and the catalyst. Here, steric considerations become important, and removal of the more sterically accessible *para* bromine is the dominant pathway. This is also consistent with the literature for reductive debromination of PBDEs and reductive dechlorination of PCBs by nZVI@Pd and similar bimetallic systems [30,48].

In the photodebromination reaction of BDE-47, a small amount of BDE-8, the product of debromination of an *ortho*-substituted bromine, was noticed after 50 h of the reaction (Fig. S2), suggesting that direct photolysis occurred as the reactivity of the photocatalyst diminished; as mentioned above, direct photolysis favors debromination at the *ortho*- over the *para*-position. No further debromination products were noticed as the reaction reached 100 h.

3.3. Reductive debromination of dibromodiphenyl ethers

To further investigate its activity, a set of experiments was conducted using the Cu$_2$O@Pd photocatalyst and each of three dibromo- daughter products of BDE-47 in which the bromines are on *ortho* or *para* orientation on different rings (BDE-4, BDE-8, and BDE-15). Fig. 3 shows the results of these reactions, in which BDE-4, BDE-8, and BDE-15 were individually treated with Cu$_2$O@Pd and exposed to light as in the BDE-47 experiments. For the BDE-15 reaction, the products were BDE-3 and the fully-debrominated diphenyl ether (DPE). The BDE-15 data show 75% removal of at least one bromine within the first 10 h of the reaction. BDE-8 gave rise to a substantial amount of BDE-1 but no BDE-3 or DPE, while BDE-4 was only slightly reactive. In the case of BDE-8, the original concentration was decreased by about 40% at 10 h with loss of its one *para*-bromine to yield BDE-1. This behavior is consistent with the previous observation (Fig. 2) that Cu$_2$O@Pd strongly favors debromination at the *para* positions; thus, the 4,4′-dibromodiphenyl ether (BDE-15) is almost completely reacted in the course of the experiment, while insignificant debromination occurs in the case of the 2,2′-congener (BDE-4). For the removal of the first bromine, the pseudo-first-order rate constant for BDE-15 (0.23 h^{-1}) is about 40-fold higher than that for BDE-4 (0.0058 h^{-1}), with BDE-8, the 2,4′-congener, being intermediate in value (0.033 h^{-1}).

3.4. Reductive debromination of the monobromodiphenyl ethers

Having established the preference for photodebromination at the *para*- *vs.* the *ortho*-position in PBDEs using Cu$_2$O@Pd, it remained to be determined what the relative activity of the catalyst is toward Br at the *meta*-position. To probe this aspect of the mechanism, a set of analogous experiments was performed with the three monobromodiphenyl ethers, BDE-1, BDE-2, and BDE-3 (Fig. 4). In all cases, the only product detected was DPE. Here, the *ortho*-brominated compound (BDE-1) shows slight reactivity, and only a trace of DPE is observed (initial pseudo-first-order rate constant k_{obs} = 0.026 h^{-1}). The *para*-brominated BDE-3 is the most reactive of the three (k_{obs} = 0.096 h^{-1}), and the *meta*-brominated BDE-2 (k_{obs} = 0.039 h^{-1}) is of intermediate activity. For BDE-3, we observe 50% debromination to DPE in the first 10 h.

Comparison of the observed rate constants for the single-*para*-Br debromination reactions may be of particular interest. The rate constants for BDE-47 and BDE-15 debromination are similar, while those for BDE-8 and BDE-3 are slower. Thus, the debromination

rates appear to be largely dependent upon the number of *para*-Br substituents, rather than the total number of bromines. This result is somewhat unexpected, since it has been generally established that the fewer the number of bromines, the more difficult it is to remove one [34]. This suggests that the catalytic mechanism is largely insensitive to the electronic environment of the bromine substituent, but depends strongly on steric effects.

3.5. Visible light reductive debromination

Cu$_2$O is a p-type semiconductor with a direct band gap of ∼2.17 eV [44,49], which corresponds to visible light at a wavelength of approximately 570 nm. To investigate the visible light activity of the Cu$_2$O@Pd nanocrystals, the aforementioned BDE-47 debromination experiments were repeated using a UV cut-off filter. Under visible light irradiation, approximately 70% of the BDE-47 was debrominated by the Cu$_2$O@Pd photocatalyst to lower-brominated congeners within the first 10 h of the reaction; the corresponding pseudo-first-order rate constant was 0.16 h^{-1} (Fig. 5). Furthermore, the products indicate that the photocatalytic reductive debromination occurs exclusively at the *para*-position, as only BDE-17 and BDE-4 are found in measureable quantity. Significantly, BDE-8 is absent from this product mixture, which suggests that BDE-8 is produced by the alternate pathway of direct photolysis by UV light in the unfiltered catalyzed reaction (Fig. S1). On the other hand, the control reaction in the absence of the Cu$_2$O@Pd materials demonstrated no degradation of BDE-47 using visible light: no photolysis products were detected, and there was no significant change in the BDE-47 concentration. The average dissociation energy reported for a phenyl C—Br bond is 84 kcal/mol [50] (which corresponds to an absorption at a wavelength of about 340 nm). Specifically for BDE-47, the maximum absorption (λ_{max}) is at 291 nm [36], and therefore direct photolysis of a BDE-47 C—Br bond requires light in the UV range. This is supported by the observation that there is almost no reaction when UV is filtered out.

3.6. Stability of the catalyst

To investigate the deterioration in catalytic activity observed after several hours of reactivity, an additional experiment was done in which BDE-47 and Cu$_2$O@Pd were exposed to light as before; then, after the reaction had slowed (50 h), an additional quantity of BDE-47 was added. This new system was then subjected to an additional 50 h of reactivity under optical illumination. In the first half of the experiment, the major product was BDE-4, consistent with the photocatalytic reductive pathway; in the latter half of the experiment, BDE-15 appeared, while the amount of BDE-4 did not increase appreciably. This suggests that after a period of time the catalyst becomes deactivated, and direct photolysis becomes favored. This conclusion is further supported by a different experiment in which addition of more catalyst at the 50 h point resulted in further product formation that was consistent with the catalytic pathway.

To explore the deactivation of the catalyst, SEM images of the Cu$_2$O@Pd multicomponent materials employed in the photocatalytic degradation of BDE-47 at different time intervals were acquired to identify changes in the particle structure. SEM analysis of the material at several stages of the reaction (Fig. 6) shows that at 5 h of reaction there are faint signs of surface pitting on the Cu$_2$O cubes. This pitting deepens over time and by 20 h is substantial. No significant further change in the morphology of the photocatalyst was noticed up to 100 h. Pitting of the material was also observed when a suspension of particles in the ethanol/water mixture without BDE was subjected to the same conditions. This indicates that the deterioration in the photocatalytic reductive debromination of PBDEs by Cu$_2$O@Pd nanomaterial can be attributed to the physical
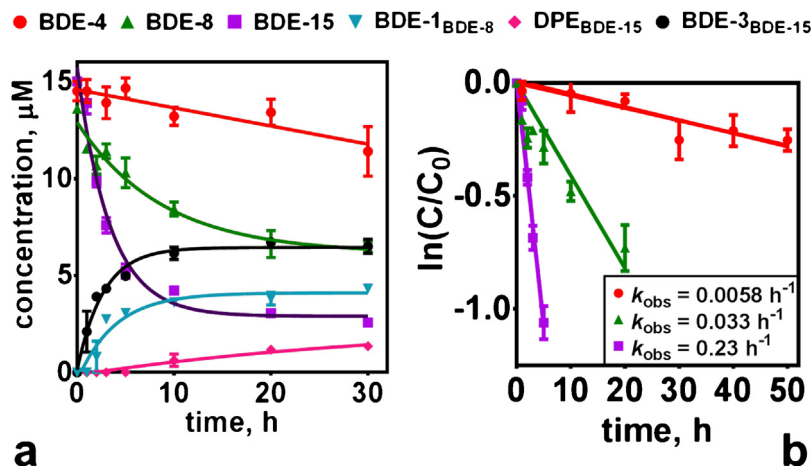
Fig. 3. Photodebromination reactions of selected dibromodiphenyl ethers under light irradiation with 1 mg/mL Cu$_2$O@Pd suspension: BDE-4, -8, and -15. (a) Concentration of BDE vs time; (b) ln (C/C$_0$) vs time; pseudo-first-order rate constants shown. BDE-1$_{BDE-4}$ refers to BDE-1 formed through debromination of BDE-4; BDE-1$_{BDE-8}$ refers to BDE-1 formed through debromination of BDE-8; BDE-3$_{BDE-15}$ refers to BDE-3 formed through debromination of BDE-15; and DPE$_{BDE-15}$ refers to DPE formed through debromination of BDE-15. Error bars represent standard error (n = 3).
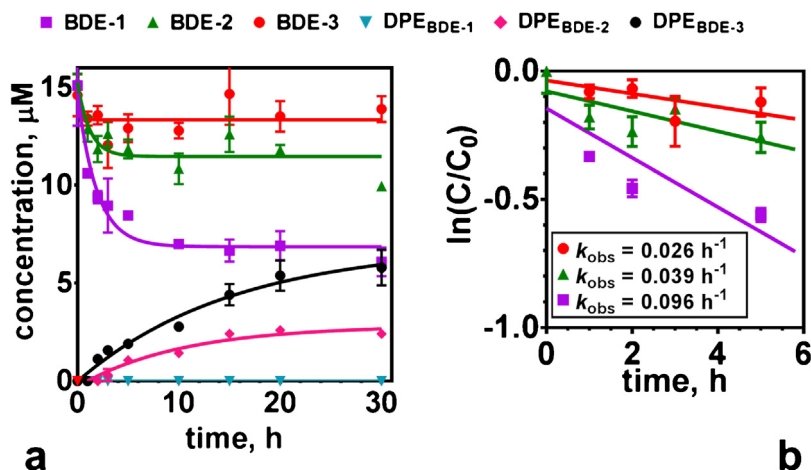

Fig. 4. Photodebromination reactions of the monobromo-DPEs under light irradiation with 1 mg/mL Cu$_2$O@Pd suspension: BDE-1, -2, and -3. (a) Concentration of BDE and DPE vs time; (b) ln (C/C$_0$) vs time; pseudo-first-order rate constants shown. Error bars represent standard error (n = 3).
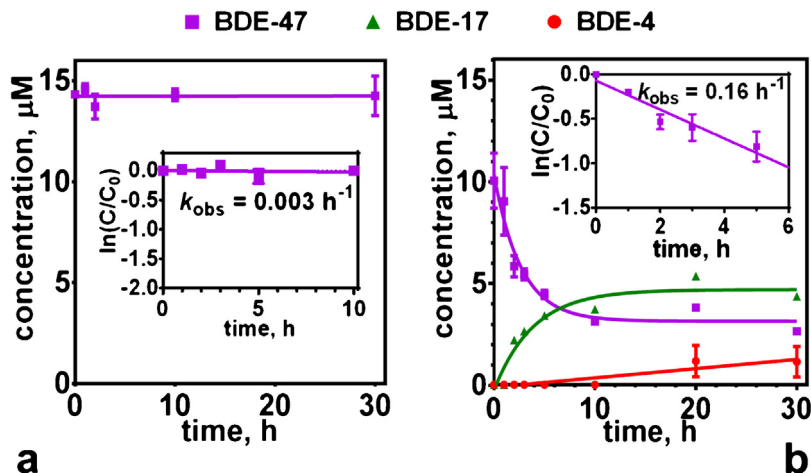

Fig. 5. Concentration of BDE components vs. time showing visible-light photodebromination reactions of BDE-47 (using UV filter, 400 nm cutoff). (a) Reaction without catalyst; (b) reaction with 1 mg/mL Cu$_2$O@Pd suspension. Insets show ln(C/C$_0$) vs time and indicate pseudo-first-order rate constants. Error bars represent standard error (n = 3).

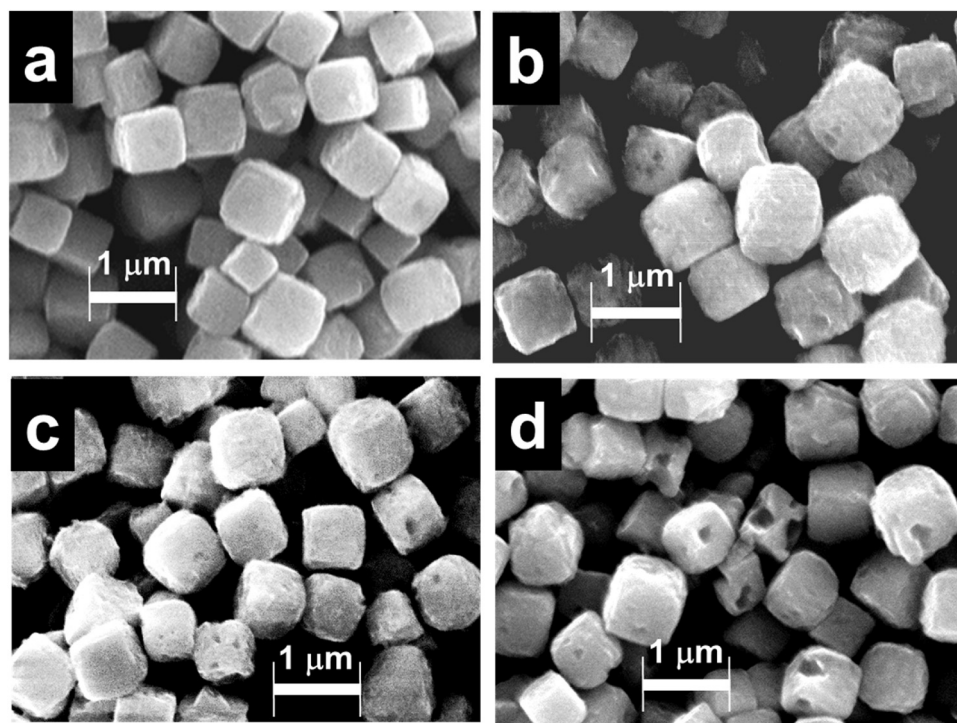**Fig. 6.** SEM images showing degradation of $Cu_2O@Pd$ catalyst as reaction proceeds: (a) 0 h, (b) 5 h, (c) 10 h, (d) 20 h.

deactivation of the catalyst. The nature of this deactivation is the objective of future research in our group.

4. Conclusions

Polybrominated diphenyl ethers are a class of persistent and environmentally ubiquitous compounds that have adverse effect on the human health and ecosystem. We have demonstrated for the first time that reductive debromination of PBDEs can be achieved via a tandem photocatalytic approach using $Cu_2O@Pd$ nanomaterial. To the best of our knowledge, this is the first-reported example of a non-titania-based metal oxide semiconductor material to be employed in the photocatalytic degradation of PBDEs. $Cu_2O@Pd$ takes advantage of the narrow Cu_2O band gap to generate H_2 from water using visible light. By incorporating palladium nanoparticles on the surface of the catalyst, $Cu_2O@Pd$ is able to activate the generated hydrogen to accomplish the reductive hydrodehalogenation of the PBDE. Since $Cu_2O@Pd$ is activated by light in the visible range, it can accomplish debromination of PBDEs using less energy than direct photolysis, which requires UV radiation to break a C–Br bond. In the latter case, debromination takes place at the thermodynamically preferred *ortho* position, where the C–Br bond is weakened by its proximity to the electron-rich oxygen of the diphenyl ether. Debromination with the tandem photocatalyst takes place via a different mechanism in which activated H_2 on the $Cu_2O@Pd$ surface reacts with the PBDE. Here, steric effects become dominant and the order of reactivity of bromine substituents is *para > meta >> ortho*. With $Cu_2O@Pd$, debromination of BDE-47 at the *para-* position takes place rapidly, leaving the *ortho*-bromines which are known to be readily debrominated by direct photolysis. The $Cu_2O@Pd$ tandem photocatalyst promises to offer significant advantages over existing methods of PBDE debromination. Combination of this reductive debromination approach and the naturally occurring direct photolysis could lead to complete mitigation of polybrominated diphenyl ethers from contaminated sites.

Appendix A. Supplementary data

Supplementary data associated with this article can be found, in the online version, at http://dx.doi.org/10.1016/j.apcatb.2017.05.020.

References

[1] U.S. EPA, An Exposure Assessment of Polybrominated Diphenyl Ethers (PBDE) (Final), U.S. Environmental Protection Agency, Washington, DC, EPA/600/R-08/086F, 2010.
[2] M. Alaee, An overview of commercially used brominated flame retardants their applications, their use patterns in different countries/regions and possible modes of release, Environ. Int. 29 (2003) 683–689.
[3] Y. Guo, S.D. Shaw, K. Kannan, Spatial and temporal trends of polybrominated diphenyl ethers, in: B.G. Loganathan, P.K.S. Lam (Eds.), Global Contamination Trends of Persistent Organic Chemicals, CRC Press, Boca Raton, FL, 2012, pp. 33–71.
[4] P.O. Darnerud, G.S. Eriksen, T. Johannesson, P.B. Larsen, M. Viluksela, Polybrominated diphenyl ethers: occurrence, dietary exposure, and toxicology, Environ. Health Perspect. 109 (Suppl 1) (2001) 49–68.
[5] M. Alaee, R.J. Wenning, The significance of brominated flame retardants in the environment: current understanding, issues and challenges, Chemosphere 46 (2002) 579–582.
[6] R.J. Law, A. Covaci, S. Harrad, D. Herzke, M.A. Abdallah, K. Fernie, L.M. Toms, H. Takigami, Levels and trends of PBDEs and HBCDs in the global environment: status at the end of 2012, Environ. Int. 65 (2014) 147–158.
[7] C.A. de Wit, An overview of brominated flame retardants in the environment, Chemosphere 46 (2002) 583–624.
[8] J.S. Park, R.W. Voss, S. McNeel, N. Wu, T. Guo, Y. Wang, L. Israel, R. Das, M. Petreas, High exposure of California firefighters to polybrominated diphenyl ethers, Environ. Sci. Technol. 49 (2015) 2948–2958.
[9] S. Ma, Z. Yu, X. Zhang, G. Ren, P. Peng, G. Sheng, J. Fu, Levels and congener profiles of polybrominated diphenyl ethers (PBDEs) in breast milk from Shanghai: implication for exposure route of higher brominated BDEs, Environ. Int. 42 (2012) 72–77.

[10] S.J. Trumble, E.M. Robinson, M. Berman-Kowalewski, C.W. Potter, S. Usenko, Blue whale earplug reveals lifetime contaminant exposure and hormone profiles, Proc. Natl. Acad. Sci. U. S. A. 110 (2013) 16922–16926.

[11] S. Hallgren, T. Sinjari, H. Hakansson, P.O. Darnerud, Effects of polybrominated diphenyl ethers (PBDEs) and polychlorinated biphenyls (PCBs) on thyroid hormone and vitamin A levels in rats and mice, Arch. Toxicol. 75 (2001) 200–208.

[12] L. Yu, Z. Han, C. Liu, A review on the effects of PBDEs on thyroid and reproduction systems in fish, Gen. Comp. Endocrinol. 219 (2015) 64–73.

[13] V.M. Richardson, D.F. Staskal, D.G. Ross, J.J. Diliberto, M.J. DeVito, L.S. Birnbaum, Possible mechanisms of thyroid hormone disruption in mice by BDE 47, a major polybrominated diphenyl ether congener, Toxicol. Appl. Pharmacol. 226 (2008) 244–250.

[14] L.G. Costa, G. Giordano, Developmental neurotoxicity of polybrominated diphenyl ether (PBDE) flame retardants, Neurotoxicology 28 (2007) 1047–1067.

[15] V. Linares, M. Belles, J.L. Domingo, Human exposure to PBDE and critical evaluation of health hazards, Arch. Toxicol. 89 (2015) 335–356.

[16] K. Walsh, EPA bans manufacture of penta- and octa-BDE, Chem. Week 166 (2004) 28.

[17] Deca-BDE to be phased out in the USA; additive producers reveal progress on alternatives, Additives for Polymers, 2010 (2010) 1–2.

[18] M.J. La Guardia, R.C. Hale, E. Harvey, Detailed polybrominated diphenyl ether (PBDE) congener composition of the widely used penta-, octa-, and deca-PBDE technical flame-retardant mixtures, Environ. Sci. Technol. 40 (2006) 6247–6254.

[19] R. Alcock, Understanding levels and trends of BDE-47 in the UK and North America: an assessment of principal reservoirs and source inputs, Environ. Int. 29 (2003) 691–698.

[20] J. Xin, X. Liu, W. Liu, X.L. Zheng, Aerobic transformation of BDE-47 by a *Pseudomonas putida* sp. strain TZ-1 isolated from PBDEs-contaminated sediment, Bull. Environ. Contam. Toxicol. 93 (2014) 483–488.

[21] S. Zhang, X. Xia, N. Xia, S. Wu, F. Gao, W. Zhou, Identification and biodegradation efficiency of a newly isolated 2,2′,4,4′-tetrabromodiphenyl ether (BDE-47) aerobic degrading bacterial strain, Int, Biodeterior. Biodegrad. 76 (2013) 24–31.

[22] M. Lu, Z.Z. Zhang, X.J. Wu, Y.X. Xu, X.L. Su, M. Zhang, J.X. Wang, Biodegradation of decabromodiphenyl ether (BDE-209) by a metal resistant strain, *Bacillus cereus* JP12, Bioresour. Technol. 149 (2013) 8–15.

[23] J. He, K.R. Robrock, L. Alvarez-Cohen, Microbial reductive debromination of polybrominated diphenyl ethers (PBDEs), Environ. Sci. Technol. 40 (2006) 4429–4434.

[24] H. Stiborova, J. Vrkoslavova, P. Lovecka, J. Pulkrabova, P. Hradkova, J. Hajslova, K. Demnerova, Aerobic biodegradation of selected polybrominated diphenyl ethers (PBDEs) in wastewater sewage sludge, Chemosphere 118 (2015) 315–321.

[25] G.Y. Xu, J.B. Wang, Biodegradation of decabromodiphenyl ether (BDE-209) by white-rot fungus *Phlebia lindtneri*, Chemosphere 110 (2014) 70–77.

[26] K.H. Kim, D.D. Bose, A. Ghogha, J. Riehl, R. Zhang, C.D. Barnhart, P.J. Lein, I.N. Pessah, *Para-* and *ortho-*substitutions are key determinants of polybrominated diphenyl ether activity toward ryanodine receptors and neurotoxicity, Environ. Health Perspect. 119 (2011) 519–526.

[27] G. Söderström, U. Sellström, C.A. de Wit, M. Tysklind, Photolytic debromination of decabromodiphenyl ether (BDE 209), Environ. Sci. Technol. 38 (2004) 127–132.

[28] Y. Zhuang, S. Ahn, R.G. Luthy, Debromination of polybrominated diphenyl ethers by nanoscale zerovalent iron: pathways, kinetics, and reactivity, Environ. Sci. Technol. 44 (2010) 8236–8242.

[29] A. Huang, N. Wang, M. Lei, L. Zhu, Y. Zhang, Z. Lin, D. Yin, H. Tang, Efficient oxidative debromination of decabromodiphenyl ether by TiO_2-mediated photocatalysis in aqueous environment, Environ. Sci. Technol. 47 (2013) 518–525.

[30] M.S. Santos, A. Alves, L.M. Madeira, Chemical and photochemical degradation of polybrominated diphenyl ethers in liquid systems—a review, Water Res. 88 (2016) 39–59.

[31] Y. Pan, D.C.W. Tsang, Y. Wang, Y. Li, X. Yang, The photodegradation of polybrominated diphenyl ethers (PBDEs) in various environmental matrices: kinetics and mechanisms, Chem. Eng. J. 297 (2016) 74–96.

[32] C. Sun, W. Chang, W. Ma, C. Chen, J. Zhao, Photoreductive debromination of decabromodiphenyl ethers in the presence of carboxylates under visible light irradiation, Environ. Sci. Technol. 47 (2013) 2370–2377.

[33] X. Zeng, P.K. Freeman, Y.V. Vasil'ev, V.G. Voinov, S.L. Simonich, D.F. Barofsky, Theoretical calculation of thermodynamic properties of polybrominated diphenyl ethers, J. Chem. Eng. Data 50 (2005) 1548–1556.

[34] E. Eljarrat, M.L. Feo, D. Barceló, Degradation of brominated flame retardants, in: E. Eljarrat, D. Barceló (Eds.), The Handbook of Environmental Chemistry, 16, 2011, pp. 187–202.

[35] U. Schenker, F. Soltermann, M. Scheringer, K. Hungerbuhler, Modeling the environmental fate of polybrominated diphenyl ethers (PBDEs): the importance of photolysis for the formation of lighter PBDEs, Environ. Sci. Technol. 42 (2008) 9244–9249.

[36] J. Eriksson, N. Green, G. Marsh, Å. Bergman, Photochemical decomposition of 15 polybrominated diphenyl ether congeners in methanol/water, Environ. Sci. Technol. 38 (2004) 3119–3125.

[37] L. Li, W. Chang, Y. Wang, H. Ji, C. Chen, W. Ma, J. Zhao, Rapid, photocatalytic, and deep debromination of polybrominated diphenyl ethers on Pd-TiO_2: intermediates and pathways, Chemistry 20 (2014) 11163–11170.

[38] M. Lei, N. Wang, L. Zhu, Q. Zhou, G. Nie, H. Tang, Photocatalytic reductive degradation of polybrominated diphenyl ethers on CuO/TiO_2 nanocomposites: a mechanism based on the switching of photocatalytic reduction potential being controlled by the valence state of copper, Appl. Catal. B 182 (2016) 414–423.

[39] Y. Lv, X. Cao, H. Jiang, W. Song, C. Chen, J. Zhao, Rapid photocatalytic debromination on TiO_2 with in-situ formed copper co-catalyst: enhanced adsorption and visible light activity, Appl. Catal. B 194 (2016) 150–156.

[40] Y. Zhuang, S. Ahn, A.L. Seyfferth, Y. Masue-Slowey, S. Fendorf, R.G. Luthy, Dehalogenation of polybrominated diphenyl ethers and polychlorinated biphenyl by bimetallic, impregnated, and nanoscale zerovalent iron, Environ. Sci. Technol. 45 (2011) 4896–4903.

[41] E.M. Zahran, D. Bhattacharyya, L.G. Bachas, Reactivity of Pd/Fe bimetallic nanotubes in dechlorination of coplanar polychlorinated biphenyls, Chemosphere 91 (2013) 165–171.

[42] R.A. Sheldon, Fundamentals of green chemistry: efficiency in reaction design, Chem. Soc. Rev. 41 (2012) 1437–1451.

[43] E.M. Zahran, N.M. Bedford, M.A. Nguyen, Y.J. Chang, B.S. Guiton, R.R. Naik, L.G. Bachas, M.R. Knecht, Light-activated tandem catalysis driven by multicomponent nanomaterials, J. Am. Chem. Soc. 136 (2014) 32–35.

[44] M. Hara, T. Kondo, M. Komoda, S. Ikeda, J.N. Kondo, K. Domen, M. Hara, K. Shinohara, A. Tanaka, Cu_2O as a photocatalyst for overall water splitting under visible light irradiation, Chem. Commun. (1998) 357–358.

[45] M. Petreas, J. She, F.R. Brown, J. Winkler, G. Windham, E. Rogers, G. Zhao, R. Bhatia, M.J. Charles, High body burdens of 2,2′,4,4′-tetrabromodiphenyl ether (BDE-47) in California women, Environ. Health Perspect. 111 (2003) 1175–1179.

[46] EFSA Panel on Contaminants in the Food Chain (CONTAM), Scientific opinion on polybrominated diphenyl ethers (PBDEs) in food, EFSA J., 9 (2011) 274.

[47] H. Liu, S. Tang, X. Zheng, Y. Zhu, Z. Ma, C. Liu, M. Hecker, D.M. Saunders, J.P. Giesy, X. Zhang, H. Yu, Bioaccumulation, biotransformation, and toxicity of BDE-47, 6-OH-BDE-47, and 6-MeO-BDE-47 in early life-stages of zebrafish (*Danio rerio*), Environ. Sci. Technol. 49 (2015) 1823–1833.

[48] B.Z. Wu, H.Y. Chen, S.J. Wang, C.M. Wai, W. Liao, K. Chiu, Reductive dechlorination for remediation of polychlorinated biphenyls, Chemosphere 88 (2012) 757–768.

[49] M.A. Nguyen, N.M. Bedford, Y. Ren, E.M. Zahran, R.C. Goodin, F.F. Chagani, L.G. Bachas, M.R. Knecht, Direct synthetic control over the size, composition, and photocatalytic activity of octahedral copper oxide materials: correlation between surface structure and catalytic functionality, ACS Appl. Mater. Interfaces 7 (2015) 13238–13250.

[50] S.J. Blanksby, G.B. Ellison, Bond dissociation energies of organic molecules, Acc. Chem. Res. 36 (2003) 255–263.